

Quantum Cascade Lasers Integrated on Silicon

Alexander Spott,¹ Jon Peters,¹ Michael L. Davenport,¹ Eric J. Stanton,¹ Chong Zhang,¹ Charles D. Merritt,² William W. Bewley,² Igor Vurgaftman,² Chul Soo Kim,² Jerry R. Meyer,² Jeremy Kirch,³ Luke J. Mawst,³ Dan Botez,³ and John E. Bowers¹

¹Department of Electrical and Computer Engineering, University of California, Santa Barbara, Santa Barbara, CA 93106, USA

²Code 5613, Naval Research Laboratory, Washington, DC 20375, USA

³Department of Electrical and Computer Engineering, University of Wisconsin, Madison, WI 53706, USA
spott@ece.ucsb.edu

1. Introduction

Silicon integration of mid-infrared (MIR) photonic devices promises to enable low-cost, compact sensing and detection capabilities that are compatible with existing silicon photonic and silicon electronic technologies. Heterogeneous integration by bonding III-V wafers to silicon waveguides has previously been used to build diode lasers integrated with silicon waveguides for wavelengths from 1310 to 2010 nm [1]. To extend this spectral range, the versatility and performance of Quantum Cascade Lasers (QCLs) at wavelengths throughout the mid-infrared range (3000-16000 nm) makes them a desirable light source for MIR silicon photonic integrated circuits.

Here we demonstrate the successful heterogeneous integration of QCLs with silicon waveguides. Tapers in the III-V mesa transfer an optical mode from the hybrid III-V/Si active region into passive silicon waveguides, and feedback is provided by reflections from both the III-V tapers and the polished passive silicon facets.

We also show initial results of the heterogeneous integration of distributed feedback (DFB) QCLs on silicon. DFB lasers are appealing for many high-sensitivity chemical spectroscopic sensing applications in need of a single frequency, narrow-linewidth MIR source. DFB QCLs are typically fabricated by etching a Bragg grating either on the laser waveguide sidewalls [2], top waveguide surface [3], or buried within the laser structure top cladding [4]. Heterogeneous integration offers the added flexibility of constructing the DFB laser by etching a shallow surface grating onto the silicon waveguide underneath the III-V mesa [5] without the need for an epitaxial regrowth step.

These heterogeneously integrated Fabry-Pérot and DFB lasers could be employed as part of a MIR photonic integrated circuit. Multiple die bondings can enable the integration of multiple QCLs for different wavelengths throughout the MIR on one silicon chip.

2. Design

The silicon waveguides were built on the silicon-on-nitride-on-insulator (SONOI) platform, which supports transmission of ~ 1.2 - 6.7 μm wavelengths [6]. This platform consists of 1.5 μm -tall silicon waveguides above a 400 nm-thick silicon nitride layer, a 3 μm -thick silicon dioxide layer, and a silicon substrate. The SONOI platform offers the additional feature of permitting the fabrication of SiN-on-SiO₂ waveguides by removing the top silicon device layer, which can transmit from ~ 0.35 - 3.5 μm .

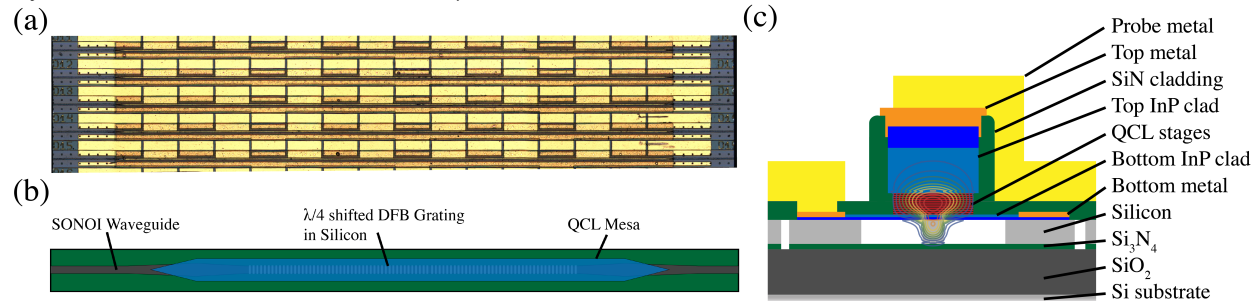


Fig. 1. (a) An optical microscope image of fully-fabricated heterogeneously integrated DFB QCLs on silicon. (b) A top-down schematic of the heterogeneously integrated DFB QCL on silicon. (c) A cross-sectional schematic of the Si/III-V active region. A simulation of the fundamental TM mode, which is shared between the silicon waveguide and III-V mesas, is overlaid.

The optical microscope image in Fig. 1(a) shows part of a laser bar with five fully fabricated QCLs on silicon. The laser design and fabrication process are similar to that of the heterogeneously integrated DFB lasers in [5] for both the Fabry-Pérot and the DFB lasers. The silicon waveguide output facets on all lasers were polished, and no coating was applied. Fig. 1(b) shows a top-down schematic of a DFB QCL on silicon consisting of a hybrid III-V/Si active region coupled to passive silicon waveguide regions on both sides with III-V tapers. Fig. 1(c) shows a cross-sectional schematic of the active region. The fabricated III-V mesa width varies from 4 - 8 μm , while the silicon waveguide width varies from 1.0 - 3.5 μm in the hybrid III-V/Si active region.

For the DFB lasers, a 28 nm-deep $\lambda/4$ shifted grating with periods between 738 and 802 nm was etched on the surface of the silicon waveguides. The III-V mesa and silicon waveguide widths define the optical mode shape, shown overlaid onto the cross-section in Fig. 1(c). The modal overlap with the active region and the grating on the silicon waveguide surface can be engineered by selection of the waveguide geometry to optimize the coupling coefficient to the grating. Simulations estimate that the confinement within the active QCL stages is from 0.6-0.75.

The QCL material with 30 stages was grown by metalorganic chemical vapor deposition (MOCVD). The design was similar to that shown in [7] and modified for flip-chip bonding for heterogeneous integration. In particular, a thin bottom InP clad and thick top InP clad were used to improve optical confinement in the silicon waveguide while preventing overlap with the top metal.

3. Results

The lasers were driven at $T = 20^\circ\text{C}$ with 250 ns pulses and a 1 kHz repetition rate. Fig. 2(a) shows the light output and voltage vs. current density of two Fabry-Pérot QCLs. The minimum threshold current density was 1.6 kA/cm^2 and the maximum output power was 31 mW. The maximum output power appears to be limited by the non-ideal coupling between the III-V and Si waveguides at the tapers as well as the stronger than intended taper reflection. Fig. 2(b) shows the relative light output and voltage for three DFB QCLs, which exhibit threshold current densities as low as 1.2 kA/cm^2 , but much lower maximum output. Emission spectra were acquired with a 0.5 m monochromator with 1.5 nm resolution. Figs. 2(c) and 2(d) show, respectively, the spectra for a Fabry-Pérot QCL with peak wavelength of $4.82\text{ }\mu\text{m}$ and a DFB QCL with peak wavelength of $4.63\text{ }\mu\text{m}$.

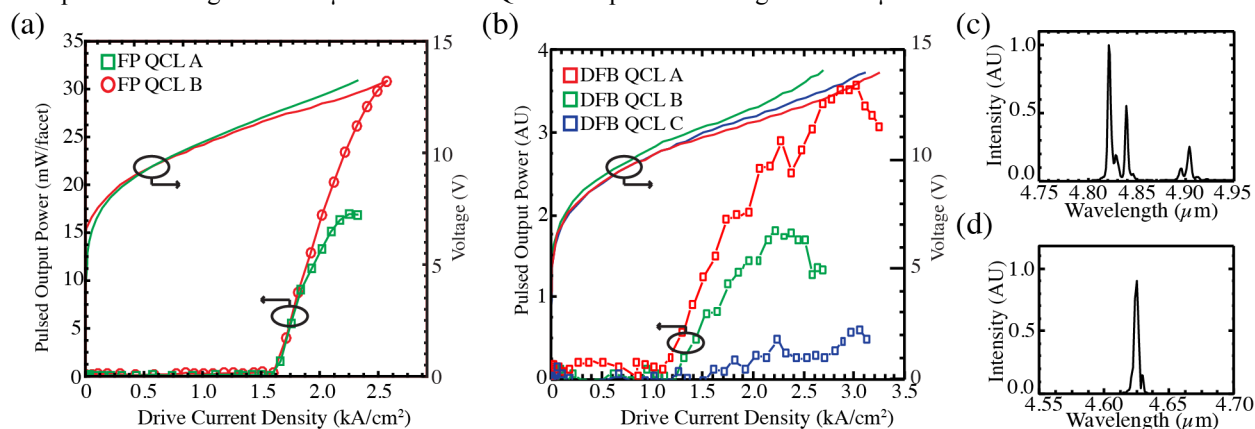


Fig. 2. (a) Single-sided output power and voltage vs. drive current density of two Fabry-Pérot (FP) QCLs on Si with $6\text{ }\mu\text{m}$ -wide III-V mesas. FP QCL A has a $1\text{ }\mu\text{m}$ -wide Si waveguide and $20\text{ }\mu\text{m}$ -long taper, while FP QCL B has a $1.5\text{ }\mu\text{m}$ -wide Si waveguide and $45\text{ }\mu\text{m}$ -long taper. (b) Relative single-sided output power and voltage vs. drive current density of three DFB QCLs on Si with $45\text{ }\mu\text{m}$ -long tapers. DFB QCL B has a $1.5\text{ }\mu\text{m}$ -wide Si waveguide and $4\text{ }\mu\text{m}$ -wide III-V mesa, while DFB QCLs A and C have $3.5\text{ }\mu\text{m}$ -wide Si waveguides and $8\text{ }\mu\text{m}$ -wide III-V mesas. (c) Emission spectrum of FP QCL B. (d) Emission spectrum of DFB QCL C.

4. Conclusion

We demonstrated QCLs heterogeneously integrated on silicon on the broadband SONOI waveguide platform. Results were presented for Fabry-Pérot QCLs and $\lambda/4$ -shifted DFB QCLs employing shallow etched gratings on the top surface of silicon waveguides.

5. References

- [1] A. Spott, M. Davenport, J. Peters, J. Bovington, M. J. R. Heck, E. J. Stanton, I. Vurgaftman, J. R. Meyer, and J. Bowers, "Heterogeneously integrated $2.0\text{ }\mu\text{m}$ CW hybrid silicon lasers at room temperature," *Opt. Lett.* **40**, 1480 (2015).
- [2] R. M. Briggs, C. Frez, C. E. Borgentun, and S. Forouhar, "Regrowth-free single-mode quantum cascade lasers with power consumption below 1 W ," *Appl. Phys. Lett.* **105**, 141117 (2014).
- [3] Q. Y. Lu, Y. Bai, N. Bandyopadhyay, S. Slivken, and M. Razeghi, " 2.4 W room temperature continuous wave operation of distributed feedback quantum cascade lasers," *Appl. Phys. Lett.* **98**, 181106 (2011).
- [4] A. Wittmann, Y. Bonetti, M. Fischer, J. Faist, S. Blaser, and E. Gini, "Distributed-Feedback Quantum-Cascade Lasers at $9\text{ }\mu\text{m}$ Operating in Continuous Wave Up to 423 K ," *IEEE Photon. Technol. Lett.* **21**, 814 (2009).
- [5] C. Zhang, S. Srinivasan, Y. Tang, M. J. R. Heck, M. L. Davenport, and J. E. Bowers, "Low threshold and high speed short cavity distributed feedback hybrid silicon lasers," *Opt. Express* **22**, 10202 (2014).
- [6] R. A. Soref, S. J. Emelett, and W. R. Buchwald, "Silicon waveguided components for the long-wave infrared region," *J. Opt. A: Pure Appl. Opt.* **8**, 840 (2006).
- [7] A. Evans, S. R. Darvish, S. Slivken, J. Nguyen, Y. Bai, and M. Razeghi, "Buried heterostructure quantum cascade lasers with high continuous-wave wall plug efficiency," *Appl. Phys. Lett.* **91**, 071101 (2007).